Theor Chem Account (2008) 120:583–589
DOI 10.1007/s00214-008-0413-z

REGULAR ARTICLE

Zn_7Cu_6: a magic cluster of brass?

Jessica Botticelli · René Fournier · Min Zhang

Received: 1 October 2007 / Accepted: 2 February 2008 / Published online: 26 February 2008

Abstract Density functional theory was applied to a series of 13-atom Zn–Cu alloy clusters. We did a thorough search for the low-energy isomers by global optimization, plus explicit optimization of all homotops of the icosahedron. Structures of copper rich clusters tend to be compact, often icosahedra, whereas zinc rich clusters ($Zn_8Cu_5^+$, Zn_9Cu_4, $Zn_{11}Cu_2$) have compact copper cores surrounded by an incomplete shell of solvating Zn atoms. The icosahedral structure, low total energy, and large hardness of Zn_7Cu_6 indicate that it has special stability among Zn_xCu_y clusters. However, Zn_7Cu_6 has many low lying isomers and a small cohesive energy compared to brass, which suggest that it is not stable in a broader sense.

Keywords Alloy clusters · Global optimization · Geometric structure · Electronic structure

1 Introduction

Cluster properties are often very different from those of the bulk material counterpart and they vary with cluster size. For example, small rhodium and manganese clusters are magnetic [1,2], nanometer sized CdS particles luminesce at different wavelengths depending on size [3], carbon nanotubes can be semiconducting or metallic depending on their geometric structure [4–9], and metal cluster reactivities can differ by orders of magnitude with addition of a few atoms [10]. This raises the prospect of making new materials with unique properties by controlled assembly of clusters having precisely defined size and composition [11,12]. This idea has been around for many years [13] but there are still few examples of true cluster assembled materials. This is because most clusters are unstable and coalesce upon condensation, or they decompose or react with ambient gases even before they can be condensed. The best hope for making cluster assembled materials rests with clusters that have a high intrinsic stability or can be passivated.

Generally, small metal clusters are very reactive and will almost surely coalesce because of the large drop in surface area, and surface energy, when two N-atom clusters combine to form a $2N$-atom cluster. However, bimetallic clusters A_xB_y could be metastable if they satisfy some stability criteria, especially if they carry surface charges that can act like a passivating coating. An example of this is Pb_4K_4 which forms a solid of Pb_4^{4-} clusters surrounded by K^+ cations [14].

Two simple models are often used to predict sizes at which metal clusters are stable relative to other clusters. The first is atomic shells [15,16]. It is based on the idea that surface energy is a key factor and packing hard spheres, one at a time, gives nonmonotonous increases in surface area. In this model, stable (or "magic") elemental clusters are part of an icosahedral growth sequence and have numbers of atoms $N_A = 13, 55, 147 \ldots$. The other model is electronic shells, which is often associated with the ellipsoidal jellium model (EJM) [17]. This predicts stable clusters when the number of delocalized electrons $N_e = 8, 20, 34, 40, 58 \ldots$. Clusters that satisfy both criteria, for example Al_{13}^- [18], are dubbed "doubly magic clusters": they should be extra stable and are interesting candidates for cluster assembled

We dedicate this manuscript to Nino Russo on the occasion of his 60th birthday.

J. Botticelli · R. Fournier (✉) · M. Zhang
Department of Chemistry, York University,
Toronto, ON, Canada M3J 1P3
e-mail: renef@yorku.ca

materials. In a theoretical study of A_4B_{12} clusters, where A is divalent and B is monovalent, we proposed a third characteristic that might give extra stability to certain clusters, namely, electrically neutral coincident electronic and nuclear shells (ENCENS) [19]. An example is Mg_4Ag_{12} which consists of a Mg_4 tetrahedron (inner shell of four +2 ions, $\sum_j Z_j = 8$) surrounded by 12 Ag atoms which makes a second ionic shell ($8+12 = 20$) thereby matching *two* electronic shell closings (8 and 20). This particular cluster isomer is apparently the global minimum of Mg_4Ag_{12} and has a very large HOMO–LUMO gap (2.46 eV in the B3LYP approximation) atypical for metal clusters.

There are many ways, of course, to make bimetallic doubly magic clusters, especially if unequal sizes of A and B allow atomic shell closings to occur at nuclearities other than 13 or 55. Among them, Zn_7Cu_6 looks especially attractive: it is small and it is close to a 50–50% mixture; Cu and Zn atomic radii are comparable but unequal, which provides a way to accomodate the strain inherent to the icosahedron; and the corresponding bulk alloy, brass, has been known since antiquity.

Modelling brass surfaces is not the main motivation for the present study. However, the cluster equilibrium structures that we report here could be useful for that purpose in the future. Therefore, a few comments about brass surfaces are in order. The word brass can refer to any alloy of Zn and Cu, but the commonly used alloys all have a Zn content below 40%. However, Zn has a much lower surface energy than Cu, so it normally segregates to the surface of a clean non-oxidized brass surface [20]. This has been observed, but measurements on non-oxidized surfaces are difficult: the precise Zn content in the few topmost layers of brass alloys varies depending on the method of sample preparation and is not known precisely [21]. The surface of typical brass samples consists of a fairly thick oxide layer. Small Zn_xCu_y clusters are very different from that. But oxide-free brass surfaces can be made by sputtering in ultra-high vacuum, and there Zn_xCu_y clusters of different compositions could serve as models for surface sites.

We investigated Zn_7Cu_6, along with a few other Zn_xCu_y ($x + y = 13$) species with even number of electrons, as a model doubly magic cluster to address a number of questions. How large is the HOMO–LUMO gap, and can the cluster still be considered metallic? Is there extra stability associated with the 20 electron count of Zn_7Cu_6? Are there surface charges on Zn_7Cu_6 that could help passivate it somehow? Is the ICO, or another quasi-spherical structure, favored? Are there distortions in Zn_xCu_y consistent with either EJM or ENCENS? Homotops are cluster isomers that have the same topology but differ in how two or more atom types are distributed among the fixed sites: which homotop, among ICO structures, is most stable, and why?

2 Methods

Density functional theory (DFT) calculations were done with the G03 software [22] using LANL2DZ effective core potential and basis sets [23] and the PBE exchange-correlation (XC) functional [24,25]. Previous studies have shown that copper and zinc clusters with more than four atoms have singlet or doublet ground states. Here we considered only species with even number of electrons and assume singlet ground states everywhere: the relatively large calculated HOMO–LUMO gaps show that this is probably correct. We did two series of calculations. First, we created initial structures for all distinct homotops of the ICO for Zn_xCu_y ($x + y = 13$ and $x = 3, 5, 7, 9, 11$), $Zn_6Cu_7^-$, and $Zn_8Cu_5^+$, and did local optimization on those. There are 8 homotops for Zn_3Cu_{10}, 21 for Zn_5Cu_8 (or $Zn_8Cu_5^+$), 28 for Zn_7Cu_6 (or $Zn_6Cu_7^-$), 15 for Zn_9Cu_4, and 4 for $Zn_{11}Cu_2$. We also did a number of local optimizations on O_h symmetry fcc fragments and found that they were all significantly higher in energy (0.5 eV or more) than the most stable ICO homotop. Second, we did a global minimization of the DFT-PBE energy by Taboo Search [26,27] in Descriptor Space (TSDS) [28,29], using G03, for all Zn_xCu_y species that appear in reactions (1) and (2). In the TSDS, 400 structures were created each of which is *near* a local minimum: most of these structures (typically more than 300) are distinct from all others, and the rest are distorted copies of the lowest energy structures. The TSDS algorithm then selects the 15 most promising candidates out of the 400, based on energy and diversity criteria, and performs local optimization for each. The GM, according to the TSDS, is the lowest energy from these 15 optimized structures. Four hundred energy-structure data followed by 15 local optimization constitutes a *very* short run for global optimization, especially considering that the number of local minima for Zn_7Cu_6 is on the order of a million. [1] However, the main purpose of the global optimization here is to get a sense for the likelihood that the GM is an ICO or a totally different kind of structure, and see how this might affect calculated relative stabilities of Zn_xCu_y species. Note also that TSDS is very efficient because it uses descriptors such as numbers of Cu–Cu, Zn–Zn and Cu–Zn neighbor pairs, and ratios of moments of inertia, to guide the search. For example, a TSDS can discover early on in a search that geometries which are very elongated (e.g., chains) or poorly mixed (with all Cu atoms on one side) have a high energy and it "learns" to avoid those structures which cuts down drastically on the number of local minima being searched. As a precaution, we repeated TSDS global optimization (for $x = 5, 7, 9$) with a different software and method—VASP

[1] The number of local minima of Ar_{13} is close to 1500, and the number of homotops of Zn_7Cu_6 is 1716 for a basic structure with no symmetry and 28 for an ICO basic structure.

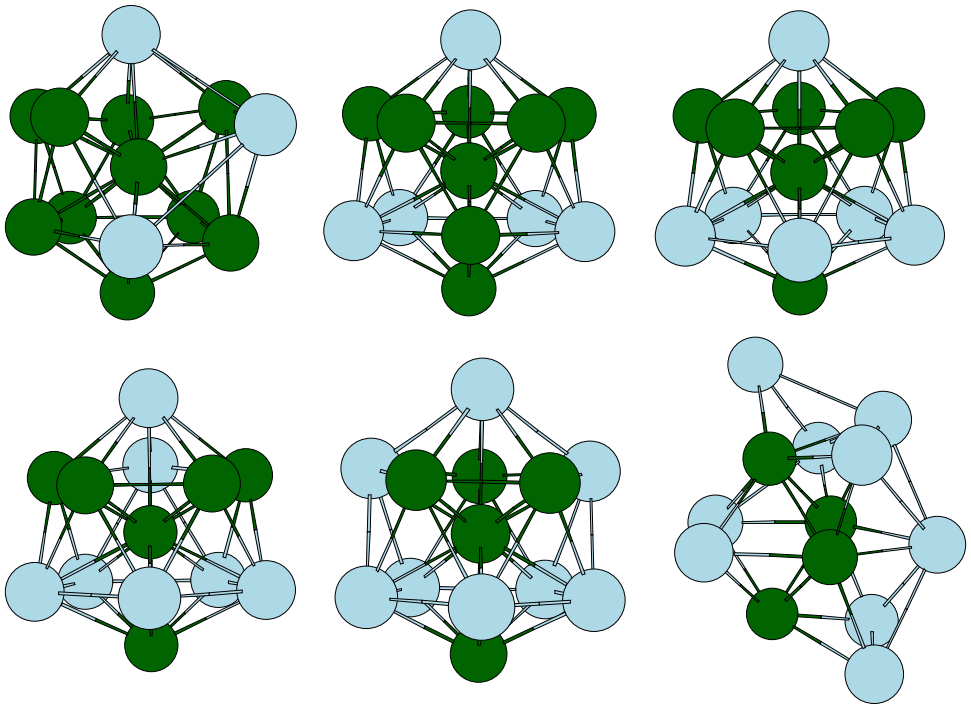

Fig. 1 Lowest energy homotops of icosahedral Zn_xCu_y clusters [x =3, 5, 6 (anion), 7, 8 (cation), 9]. *Light shaded circles* depict Zn atoms

[30–32] with the plane augmented wave (PAW) method and PBE XC. We also did fixed nuclei calculations (PBE optimized geometries) with the B3LYP [33] XC functional in order to calculate more realistic HOMO–LUMO gaps [34]. As a test we did a few B3LYP geometry optimizations to see the effect of changing XC on geometries. In order to characterize the shape of clusters, we calculated a descriptor

$$\eta = (2I_b - I_a - I_c)/I_a$$

where $I_a > I_b > I_c$ are moments of inertia calculated using a fictitious unit mass for Cu and Zn atoms. Note that η is zero for an ideal icosahedron.

3 Results

3.1 Icosahedral homotops

The lowest energy ICO homotop (ICO-GM) of each species are shown in Fig. 1 and their properties are in Table 1. The ICO structure is distorted but still well defined after local optimization by PBE in all cases except Zn_9Cu_4. Many of the B3LYP structures (not shown here) become strongly distorted following optimization of an initial ICO. In a study of first-row transition metal diatomics [35,36], Barden et al. found that a generalized gradient approximation functional gave bond lengths and vibrational frequencies in better agreement with experiment than B3LYP. In a recent study of the performance of different functionals for bulk solids, Paier et al. [37] showed that B3LYP gives much larger errors than PBE on lattice constants, bulk modulus, and atomization energies of metals, in particular, transition metals. They concluded that B3LYP is "not capable to describe the transition from a localized to an itinerant behavior". We believe that a PBE treatment of exchange-correlation gives more reliable structures and energies of metal clusters than B3LYP and here we base most of our discussion on PBE results.

It would be impractical to show all homotops so we devised a system for giving them unique names. Each name consists of a "c" or "z", depending on the central atom (Cu or Zn),

Table 1 Properties of the lowest energy structure (GM) of each species: total energy (TE), HOMO-LUMO gap (HLG), cohesive energy (CE in eV/atom), ionization energy (IE), electron affinity (EA), and shape parameter η

	TE (au)	CE	HLG (eV)	IE (eV)	EA (eV)	η
Zn_3Cu_{10}*	−2,159.5957	1.922	0.48	5.78	2.02	−0.06
Zn_3ICO	−2,159.5949	1.919	0.65	6.05	2.07	−0.09
Zn_5Cu_8	−1,899.1113	1.680	0.58	6.13	2.25	−0.05
Zn_7Cu_6	−1,638.6087	1.399	1.25	5.93	1.40	−0.02
Zn_9Cu_4*	−1,378.0828	1.070	1.29	5.64	1.30	+0.28
$Zn_6Cu_7^-$	−1,768.9496	1.669	(1.5)	–	–	0.00
$Zn_8Cu_5^+$*	−1,508.1611	1.451	1.30	–	–	−0.07
$Zn_8Cu_5^+$ICO	−1,508.1413	1.409	1.17	–	–	−0.01

Non-ICO clusters are indicated by an asterisk. The ground state energies of atomic species are: Cu −196.094645; Cu^+ −195.806618; Cu^- −196.122214; Zn −65.910351; Zn^+ −65.580133

followed by a sequence of K numbers n_j ($j = 1, K, 1 \leq K \leq 6$). Each number n_j is associated to one surface atom of type "A", where "A" is the element in minority on the surface of the ICO: n_j is the number of A-type surface atoms that are a neighbor of that atom. The n_js are listed by groups of connected atoms, starting with the largest group. Within each group, n_js are given for a sequence of neighbors such that the largest n_js appear early in the sequence. A slash is put between n_js of non-neighboring atoms belonging to the same group when it is impossible to express all atoms of that group as a sequence of neighbors, for example, z1331/31.[2]

The ICO-GM structures in Fig. 1a–e are named c121, c1221-0, c22222-0, c1221-0, and c11-0-0. They are characterized by a central Cu atom and a small value of $N = \sum_j n_j$, i.e., good mixing of Cu and Zn atoms. It is not surprising that homotops with central Cu atom are more stable. The Cu atom's smaller size helps relieve the radial strain of the ICO somewhat, and bulk Cu has a higher surface energy (and higher cohesive energy) than bulk Zn so, generally, Zn should segregate to the surface of ZnCu alloy clusters. Mixing, on the other hand, increases the ionic contribution to energy. This energy term must be small because the absolute electronegativities, (IE+EA)/2, where IE is the ionization energy and EA is the electron affinity, of Cu and Zn atoms are very similar, 4.48 and 4.70 eV, respectively. But they are still large enough to account for energy differences of a few tenths of eV between homotops.

Table 2 shows various properties of the 28 ICO homotops of Zn_7Cu_6 listed in increasing order of their energy. The names of homotops themselves show that the energetic preference for a central Cu atom and small $N = \sum_j n_j$ is not limited only to the GM, it is rather general. The relative energies (PBE) show three Cu-centered homotops within 0.1 eV of each other. Experiments on Zn_7Cu_6 would probably measure thermally averaged properties over these homotops. The B3LYP predictions are quite different from PBE: on average the two sets of REs differ by 0.25 eV. The two most stable homotops in B3LYP each are different from the three most stable homotops in PBE. Both theories predict that Cu-centered homotops are (almost always) more stable. The PBE HOMO-LUMO gaps (1.3 eV for the most stable homotops) are quite large compared to metal clusters of that size. The B3LYP gaps are bigger: they vary between 1.58 and 2.16 eV for "c" homotops. There is a moderate correlation between gap and energy, consistent with the maximum hardness principle [38–41], but only if we look at "c" and "z" homotops separately: then, correlation coefficients are 0.56 and 0.84, respectively.

[2] If we project the six A surface atoms of the z1331/31 homotop on a plane, we get an equilateral triangle of atoms with three singly coordinated capping atoms: it is impossible to step through each of those six atoms exactly once by following a sequence of neighbours.

Table 2 Properties of the lowest-energy icosahedral homotops of Zn_7Cu_6 calculated by PBE: relative energy (RE, in eV), HOMO-LUMO gap (eV), dipole moment (μ, in Debye), and separation of Zn_x and Cu_y centers of mass (S, in Å)

	RE		gap	μ	S
	PBE	B3LYP			
c1221-0	0.00	0.21	1.26	0.16	0.91
c22222	0.03	0.31	1.34	0.48	1.70
c13231	0.06	0.35	1.25	0.41	1.71
c12221	0.21	0.53	0.99	0.31	1.08
c121-11	0.22	0.63	0.95	0.16	0.43
c42332	0.22	0.53	1.15	0.47	2.28
c22321	0.25	0.11	0.98	0.41	1.46
c2231-0	0.27	0.35	0.97	0.16	1.13
c3232-0	0.34	0.00	0.89	0.34	1.55
c222-11	0.35	0.40	1.18	0.15	0.96
c32331	0.35	0.77	0.92	0.35	1.84
z22222-0	0.54	0.77	1.72	0.31	1.02
z1331/31	0.56	0.75	1.73	0.45	1.45
z233222	0.67	0.80	1.37	0.64	1.62
z244242	0.71	0.86	1.62	0.71	2.39
z122221	0.72	0.58	1.32	0.22	0.52
z132321	0.74	0.65	1.29	0.51	1.18
z243331	0.76	0.56	1.33	0.69	1.93
z533333	0.78	0.93	1.57	0.81	2.64
z432432	0.81	0.56	1.30	0.77	2.19
z222222	0.83	0.61	1.13	0.61	0.91
z42332-0	0.84	0.78	1.26	0.46	1.62
z323321	0.90	0.40	1.08	0.56	1.41
z223322	0.90	0.77	1.08	0.48	1.31
z223221	0.94	0.70	1.10	0.27	0.82
z133331	1.00	1.40	1.10	0.41	1.36
z3232-11	1.05	1.45	1.00	0.26	0.90
z222-222	1.36	1.92	0.70	0.07	0.00

The segregation parameter "S" in Table 2 is the distance, in Å, between the centers of mass of the two groups of atoms (Zn_7 and Cu_6). It gives a way to quantify mixing that is complementary to N. It correlates well with dipole moment μ, as expected (correlation coefficient of 0.74), but does not correlate with energy. Curiously, we found only a very weak correlation between S and μ for the ICO homotops of Zn_5Cu_8 and Zn_9Cu_4.

3.2 Global minima

3.2.1 Zn_3Cu_{10}

Global minimization yielded many minima with energies comparable to the ICO-GM, see Fig. 2. The lowest of these

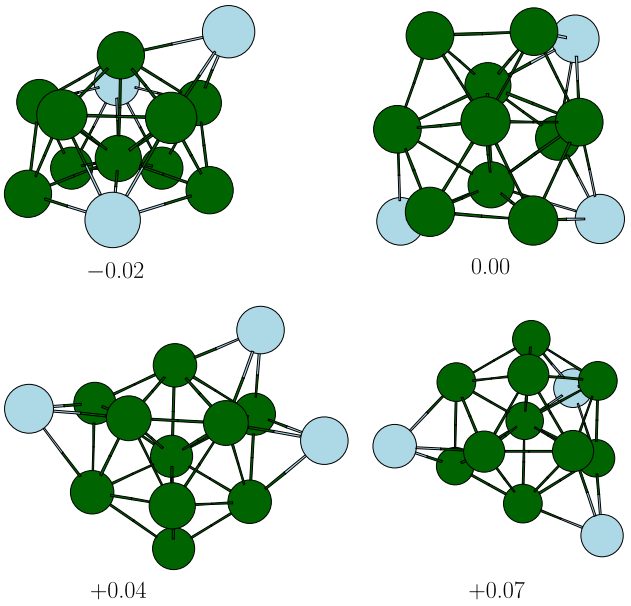

Fig. 2 Lowest energy Zn_3Cu_{10} structures found by global optimization and their energy (eV) relative to the lowest ICO structure

is in fact more stable than the ICO-GM by 0.02 eV and therefore is our predicted global minimum. The other structures in Fig. 2 are all more stable than the second most stable ICO homotop. Their energies, relative to the ICO-GM, are 0.00, +0.04, and +0.07 eV.

3.2.2 Zn_5Cu_8

The TSDS optimization reproduced the ICO-GM in both runs (G03 and VASP) so this is our proposed global minimum. No other structure was found close in energy. The second most stable structure found by TSDS is a icosahedral cage with a exohedral Cu atom: it is 0.25 eV higher than the ICO-GM.

3.2.3 Zn_7Cu_6

The TSDS found the ICO-GM c1221-0 as the most stable structure. It also produced the close-lying ICO c13231 at +0.06 eV, but did not find c22222 which lies at +0.03 eV. Other structures found by TSDS were more than 0.2 eV above the GM. This suggests that the GM is indeed an ICO (c1221-0) but also shows the limited ability of very short TSDS runs to discover low-energy isomers.

3.2.4 Zn_9Cu_4

Global optimization failed to discover any of the three lowest ICO. The lowest energy structure found is a Cu centered ICO c0-0-0 where a Zn atom has been moved to a Cu capping position. This is 0.39 eV above the GM of Fig. 1. Curiously, local optimization starting with c0-0-0 yields a structure that is 0.81 eV above the GM.

3.2.5 $Zn_{11}Cu_2$

We only considered the ICO homotops of $Zn_{11}Cu_2$ (no global optimization), but the GM of $Zn_{11}Cu_2$ is almost surely *not* an ICO: Zn_9Cu_4 is very distorted relative to an ideal ICO and we found the ICO is 0.5 eV above the GM for Zn_{13} [42]. The most stable of the four ICO homotops of $Zn_{11}Cu_2$ is the Cu-centered one. It is strongly distorted: the two Cu atoms form a dimer that is displaced so that the center of mass of the cluster is close to the Cu–Cu midpoint and the symmetry remains approximately C_{5v}.

3.2.6 $Zn_6Cu_7^-$

Global optimization gave the ICO c122221 (+0.16 eV above GM) and ICO c132321 (+0.21 eV above GM). The series of local optimization we did showed that, in addition to the GM, three other homotops have comparable or smaller RE (+0.03, +0.19, +0.20 eV). Failure to find the GM shows that our TSDS run was too short, but the fact that the best structures found by TSDS are all ICO is reassuring.

3.2.7 $Zn_8Cu_5^+$

Global optimization gave two lower energy minima than the lowest ICO homotop, as shown in Fig. 3. Their energy, relative to ICO c11-0-0 are −0.54 eV and −0.37 eV. They appear very open but their shape parameters η (−0.07 and +0.07, respectively) are not too far from zero. We calculated atomic coordinations based essentially on a distance criterion, i.e., two atoms are considered to be neighbours if their distance is less than 1.2 times the sum of their atomic radii. The mean coordination in the three structures of $Zn_8Cu_5^+$ shown in Figs. 1 and 3 are 6.0 (ICO), 4.2 (GM) and 3.8. These suggest that pair interactions are maximized (or, surface energy is minimized) in the ICO and that the ICO should be more stable, but it is not. However, Cu has a much higher

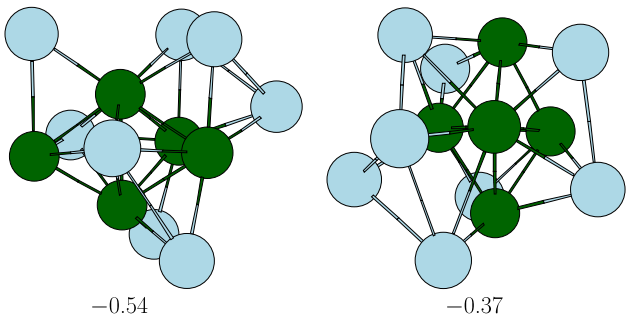

Fig. 3 Lowest energy $Zn_8Cu_5^+$ structures found by global optimization and their energy (eV) relative to the lowest ICO structure

cohesive energy than Zn (3.49 vs 1.35 eV/atom), so it is more important to achieve high coordination on Cu atoms. If we look only at Cu atoms, mean coordinations are nearly equal between the three structures: 7.1 (ICO), 7.1 (GM) and 6.9. The root-mean-square deviations (RMSD) of individual Cu atom coordinations from those averages are, for the three clusters: 2.38 (ICO), 1.31 (GM), and 1.03. This is consistent with a trend we saw in other cases [41,42], namely: everything else being equal, clusters tend to adopt structures that equalize atomic coordinations.

The comment we just made about $Zn_8Cu_5^+$ also applies to Zn_9Cu_4. The mean coordination of Cu atoms and their RMSD from the mean are 7.5 and 2.60 for an ideal Cu centered ICO, and 7.0 and 0.71 for the highly distorted GM structure of Fig. 1. In other words, distortion of the ideal ICO achieves a much smaller RMSD of Cu atom coordinations at the expense of a slight decrease of the mean coordination. So it appears that the structures of Zn-rich Zn_xCu_y obey two structural principles: they have a tendency to maximize the number of Cu–Cu bonds while simultaneously keeping nearly equal coordinations among Cu atoms. We conjecture that this generally applies to A_xB_y clusters whenever A has a much higher cohesive energy than B. If so, one expects low-symmetry solvated A_x core structures in B-rich A_xB_y clusters, whereas A-rich A_xB_y clusters should adopt more compact quasi-spherical structures.

3.3 Trends

The number of ICO homotops and other isomers that we found within 0.2 eV (PBE energies) of the GM are: 7 for Zn_3Cu_{10}, 9 for Zn_5Cu_8, 3 for Zn_7Cu_6, 5 for $Zn_6Cu_7^-$, 1 for $Zn_8Cu_5^+$, and 2 for Zn_9Cu_4. There is a lot of uncertainty on these numbers. They could be too large if we missed the GM. On the other hand, in global optimizations like TSDS it is even more likely to miss low-energy isomers other than the GM, so the numbers could be too small. And of course all these results may change if we use another XC functional. But genereally speaking, the number of low-lying isomers being 4 or 5 on average tells us that these clusters are not "magic" in the sense of having a well-defined and unique structure like, say, C_{60}. It also carries a warning about interpreting experiments on alloy clusters: measured properties are likely to be an average over two or more isomers, even when a cluster is magic in the sense of being stable relative to other related clusters, and having a large IE, small EA, comparatively low reactivity, etc.

Deviations of η from zero for the ICO-GM of Fig. 1 are as expected from the EJM: very small when the number of valence electrons $N_e = 20$, negative (oblate) when $N_e = 16$ or 18, and positive (prolate) for $N_e = 22$. The GM and low-lying isomers of Zn_3Cu_{10} in Fig. 2 also follow the rule except for the third one (with RE $= +0.04$ eV): they have $\eta = -0.06, -0.12, +0.05$ and -0.14, respectively.

If there is an energetic preference for ENCENS that causes distortion of Zn_7Cu_6, then we should expect gaps in nuclear distances to the center of ionic charge as $Z = \sum_j Z_j^{\text{ion}}$ reaches values that correspond to closed electronic shells, i.e., 2, 8, (18), 20, (34), 40…. The distances of nuclei to the center of ionic charge in the Zn_7Cu_6 c1221-0 homotop, with corresponding ion charge sums Z in parentheses, are: 0.087 (1), 2.355 (2), / 2.476 (3), 2.476 (4), / 2.562 (5), 2.562 (6), 2.605 (8), / 2.669 (10), 2.669 (12), 2.706 (14), 2.781 (16), 2.781 (18), / 2.926 (20). The gaps larger than 0.05 Å are at Z=1, 2, 4, 8, 14, and 18. Gaps at 2, 8, and 18 match the EJM-ENCENS model, but the other three do not. A similar analysis for other GM structures gives little support for ENCENS. So we conclude that the hypothetical effect of ENCENS on geometric structure is small or non-existent in Zn_xCu_y.

The reactions in Eqs. 1–4 are all calculated to be endothermic, by 0.32, 0.59, 0.71, and 1.31 eV, respectively.

$$Zn_7Cu_6 \rightarrow \frac{1}{2}(Zn_5Cu_8 + Zn_9Cu_4) \quad (1)$$

$$Zn_7Cu_6 \rightarrow \frac{1}{3}(Zn_3Cu_{10} + 2Zn_9Cu_4) \quad (2)$$

$$Zn_7Cu_6 \rightarrow \frac{1}{3}(Zn_{11}Cu_2 + 2Zn_5Cu_8) \quad (3)$$

$$Zn_7Cu_6 \rightarrow \frac{1}{2}(Zn_3Cu_{10} + Zn_{11}Cu_2) \quad (4)$$

The last two numbers are not very reliable because we do not have the GM of $Zn_{11}Cu_2$. Still, these energies of reaction clearly show the special stability of Zn_7Cu_6 within the Zn_xCu_y series. The HOMO–LUMO gaps also show the same. Aside from Zn_9Cu_4, the 20 electron species have a larger gap than other Zn_xCu_y species. Note that the gap calculated for $Zn_6Cu_7^-$ is not reliable because the LUMO energy is positive, that is why we put that value in parentheses in Table 1. Finally, the hardness (IE−EA)/2 is largest for Zn_7Cu_6, it is 2.265 eV. A clear anti-correlation has been observed between hardness and chemical reactivity in many cluster studies [10]. The large hardness of Zn_7Cu_6 suggests that it is chemically inert relative to other metal clusters.

Mulliken charges are large and positive on the central Cu atom of the Zn_7Cu_6 GM, negative on surface Cu atoms, and small and positive (roughly +0.1) on surface Zn atoms. The Zn atoms are furthest from the center of mass, so potential reaction partners will "see" Zn atoms first. These Zn atoms are almost neutral, so they would not help to passivate Zn_7Cu_6. Better charge analyses are possible, but they would likely not change this conclusion: Zn_7Cu_6 is clearly not passivated the way ionic clusters, like Pb_4K_4, are. Furthermore, the cohesive energies that we calculate for the different Zn_xCu_y clusters vary between roughly 50 and 65%

of the value of the corresponding bulk alloy: this is small and indicates a large driving force for clusters to coalesce.

4 Concluding remarks

Among the clusters studied, all of which have even numbers of electrons, we found an ICO GM structure in Zn_7Cu_6, $Zn_6Cu_7^-$, and Zn_5Cu_8 and non-ICO GM for the others. Low-lying isomers (within 0.2 eV) are found in all cases. Deformations in the shapes (η) of the GM are consistent with the EJM but not with ENCENS. The maximum hardness principle applies rather well: HOMO–LUMO gaps and energies correlate.

The hardness of Zn_7Cu_6 (2.27 eV) suggests that it is relatively inert. The large endothermic energies of reactions and compact quasi-spherical structure of Zn_7Cu_6 also point to a special stability, at least relative to other Zn_xCu_y species. Other 20-electron Zn_xCu_y species, for example Zn_4Cu_{12} [19], could also exhibit special stability in that sense. But Zn_7Cu_6 lacks some of the characteristics normally associated with a magic cluster: it has many low-lying isomers, its cohesive energy is far below the bulk limit, and its surface atoms are not passivated. So it seems unlikely that Zn_7Cu_6 could be stable in a general sense or that it could be used as a building block for materials. However, Zn_xCu_y clusters are interesting model systems for many reasons: the complex interplay of physical effects associated with atomic and electronic shells; the very different cohesive energies which lead to qualitatively different structural and physical properties for Zn rich vs Cu rich clusters; complexities associated with homotops at different mixing ratios; and the possibility of high relative stability for magic clusters that satisfy two or more stability criteria. We believe that experimental studies of the properties—abundance, reactivity, IEs and EAs, etc.—of these small clusters of brass would be worthwhile.

Acknowledgments This work was supported by the Natural Sciences and Engineering Research Council of Canada. Some calculations were done with the facilities of the Shared Hierarchical Academic Research Computing Network (SHARCNET: www.sharcnet.ca).

References

1. Cox AJ, Louderback JG, Bloomfield LA (1993) Phys Rev Lett 71:923
2. Knickelbein MB (2001) Phys Rev Lett 86:5255
3. Alivisatos AP (1996) J Phys Chem 100:13266
4. Mintmire JW, Dunlap BI, White CT (1992) Phys Rev Lett 68:631
5. Hamada N et al (1992) Phys Rev Lett 68:1579
6. Rinzler AG et al (1995) Science 269:1550
7. Tans J et al (1997) Nature 386:474
8. Dillon AC et al (1997) Nature 386:377
9. Collins PC et al (2001) Science 292:292
10. Knickelbein MB (1999) Annu Rev Phys Chem 50:79
11. Kim S-H, Medeiros-Ribeiro G, Ohlberg DAA, Stanley Williams R, Heath JR (1999) J Phys Chem 103:10341
12. Ugrinov A, Sevov SC (2003) Inorg Chem 42:5789
13. Andres RP et al (1989) J Mater Res 4:704
14. Alonso JA (2005) Structure and properties of atomic nanoclusters imperial college press, London, pp. 371–375
15. Farges J, De Feraudy MF, Raoult B, Torchet G (1983) J Chem Phys 78:5067
16. Martin TP (1996) Phys Reports 273:199
17. Knight WD, Clemenger K, DeHeer WA, Saunders WA, Chou MY, Cohen ML (1984) Phys Rev Lett 52:2141
18. Leuchtner RE, Harms AC, Castleman AW Jr (1989) J Chem Phys 91:2753
19. Sun Y, Fournier R (2007) Phys Rev A 75:063205
20. Somorjai GA (1994) Introduction to surface chemistry and catalysis. Wiley, New York
21. Van Ooij WJ (1977) Surface Technol 6:1
22. Frisch MJ et al. (2004) Gaussian 03, Revision C.02, Gaussian, Wallingford
23. Dunning TH Jr, Hay PJ (1976) in modern theoretical chemistry, Schaefer III HF (ed) Plenum, New York, vol. 3, p 1
24. Perdew JP, Burke K, Ernzerhof M (1996) Phys Rev Lett 77:3865
25. Perdew JP, Burke K, Ernzerhof M (1997) Phys Rev Lett 78:1396
26. Cvijovic D, Klinowski J (1995) Science 267:664
27. Hong SD, Jhon MS (1997) Chem Phys Lett 267:422
28. Cheng J, Fournier R (2004) Theor Chem Acc 112:7
29. Cheng JBY (2002) MSc Thesis, York University; Fournier R (2007) J Chem Theor Comp 3:921
30. Kresse G, Furthmüller J (1996) Comput Mater Sci 6:15
31. Kresse G, Furthmüller J (1996) Phys Rev B 54:11169
32. Kresse G, Hafner J (1993) Phys Rev B 48:13115
33. Becke AD (1993) J Chem Phys 98:5648
34. Muscat J, Wander A, Harrison NM (2001) Chem Phys Lett 342:397
35. Barden CJ, Rienstra-Kiracofe, Schaefer HF III (2000) J Chem Phys. 113:690
36. Yanagisawa S, Tsuneda T, Hirao K (2000) J Chem Phys 112:545
37. Paier J, Marsman M, Kresse F (2007) J Chem Phys 127:024103
38. Pearson RG (1968) J Chem Ed 45:981
39. Parr RG, Chattaraj PK (1991) J Am Chem Soc 113:1854
40. Ayers PW, Parr RG (2000) J Am Chem Soc 122:2010
41. Fournier R (2001) J Chem Phys 115:2165
42. Sun Y, Zhang M, Fournier R (2008) Phys Rev B (in press)